J Mater Sci

Polymers & biopolymers

Black sand as source of catalysts that selectively isomerize α- and β-pinene epoxides

Luis Fernando Valencia[1] and Aída Luz Villa[1,*]

[1] *Environmental Catalysis Research Group, Chemical Engineering Department, Engineering Faculty, Universidad de Antioquia UdeA, Calle 70 No. 52-21, Medellín, Colombia*

Received: 24 December 2024
Accepted: 26 May 2025

© The Author(s), 2025

ABSTRACT

Black sand (TBS), that is a mining waste, was treated by several procedures for obtaining materials that were tested as catalysts for isomerization of α- and β-pinene epoxides. The materials were obtained by milling (IC), heat treatment (CTT_800) and hydrothermal reaction with H_2SO_4 (CAT_400). Characterization analysis included NH_3-TPD, XRD, Raman, FTIR-pyridine, XPS, and SEM–EDX. The presence of hematite, ilmenite and rutile was identified by XRD and Raman analysis. FTIR-Py analysis showed only the presence of Lewis sites for CTT_800 and CAT_400, sites that favor aldehyde formation from monoterpene epoxide isomerization. The measured acid content was 364, 316, 214, and 167 $\mu mol_{NH3/g}$ for CAT_400, CTT_800, IC, and TBS, respectively; the increase of acidity was related with a higher content of hematite and rutile phases after treatment of the mining waste. Fe, Ti, and O were identified as the main elements of the solids; no S was detected neither by FTIR, nor by XPS analysis. Over CAT_400 catalyst, α-pinene conversion and campholenic aldehyde selectivity were 96% and 64%, respectively. In the case of β-pinene epoxide isomerization, substrate conversion was 98% and myrtanal selectivity was 92%. For reusing tests, several catalyst treatments were evaluated. After five reuses of CAT_400 for α- and β-pinene epoxide isomerization, selectivity did not change but conversion decreased, which was related to the decrease of strong acid sites and hematite and/or rutile content variation; a good procedure for catalyst activation is the treatment at 300 °C.

Introduction

Black sand deposits are sources of minerals of economic and strategic interest such as magnetite, monazite, rutile, zircon, ilmenite, among others. Ilmenite ($FeTiO_3$) is a trigonal rhombohedral mineral that presents weak magnetism and contains mainly TiO_2 (49.9%) and Fe_2O_3 (39.2%) [1]; its crystal structure makes Fe and Ti easily exposed on the mineral surfaces during dissociation. Several processes have been

Handling Editor: Maude Jimenez.

Address correspondence to E-mail: aida.villa@udea.edu.co

https://doi.org/10.1007/s10853-025-11056-5
Published online: 23 July 2025

reported for ilmenite treatment, such as calcination and digestion with sulfuric acid. Ilmenite calcined at 800 °C in the presence of air is transformed into hematite, magnetite and rutile [2]. The solid obtained from ilmenite digestion with sulfuric acid contains iron sulfate and titanyl sulfate that can be hydrolyzed and calcined to obtain titanium dioxide [3]. Additionally, ilmenite is used in the production of ferrotitanium alloy, which is known as hydrogen storage and deoxidizing material [4], and in chemical loop combustion reactions because of its capacity as oxygen carrier [5]. Moreover, since ilmenite is mainly composed of iron and titanium, it is a promising material to be used as a heterogeneous catalyst in advanced oxidation reactions, due to its capacity as a photocatalyst [6]. Although the ilmenite has been used as a catalyst for several reactions, it has not been tested for the catalytic transformation of terpenes.

Terpenes can be transformed into commercially important compounds that are used to produce fragrances, perfumes, flavors, and pharmaceuticals. The monoterpenes α- and β-pinene are bicyclic compounds extracted from various essential oils such as pine and eucalyptus resins; due to the C–C double bond, it can be transformed into high value-added products that are used as intermediates in the pharmaceutical and fragrance industries [7– 9]. α-Pinene epoxide can be transformed with acid catalysts into different high value-added compounds for the flavor and pharmaceutical industries, e.g., campholenic aldehyde used for the manufacture of sandalwood-like fragrances, such as Sandalore (Givaudan), Bacdanol (IFF) and Brahmanol (Dragoso), Polysantol (Firmenich) [10]. Other products that can be obtained from α-pinene epoxide include pinocarveol, *cis*-carveol, and *p*-methadien-2-ol (Fig. 1); furthermore, myrtanal, myrtenol, and perillyl alcohol can be obtained from isomerization of β-pinene epoxide (Fig. 2) [11, 12]. The isomerization of α- and β-pinene epoxides and their selectivity are affected mainly by the type of acidity (Lewis or Brønsted) and the polarity of the solvent [8]. Isomerization of α-pinene epoxide with high selectivity toward campholenic aldehyde is obtained when catalysts with Lewis acid sites are used. Moreover, the type of solvent influences the formation of the products because campholenic aldehyde is favored by apolar solvents, and carveol is formed in the presence of basic polar solvents [13, 14]. The isomerization of β-pinene oxide to myrtanal is favored by the presence of Lewis acid sites, whereas Brønsted acid sites promote mainly perillyl alcohol and myrtenol [14].

Table S1 shows reported heterogeneous catalytic systems for the isomerization of α-pinene epoxide. In most of the cases, α-pinene epoxide conversion is higher than 60%, except in the case of cupper supported catalysts [9, 15]. Campholenic aldehyde is selectively produced at temperatures lower than 80 °C and in the presence of solvents as toluene [9, 15–17], dioxane [18], dichloroethane [18–20], cyclohexane [21, 22]. Furthermore, high carveol selective has been reported at temperatures above 120 °C and in the presence of N,N-dimethylacetamide, a polar protic solvent; the reported catalysts are: Sn/SiO_2 (100% conversion, 70% selectivity) [23], sulfonic acid functionalized carbon

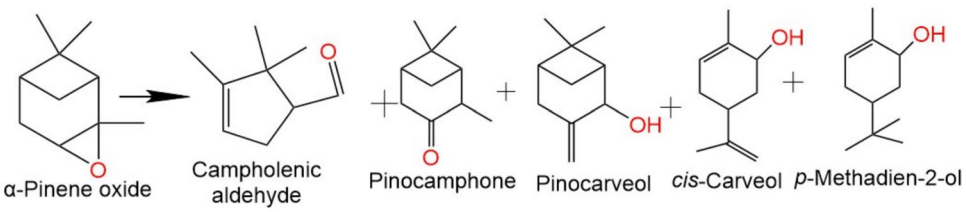


Figure 1 Main products from α-pinene epoxide isomerization.

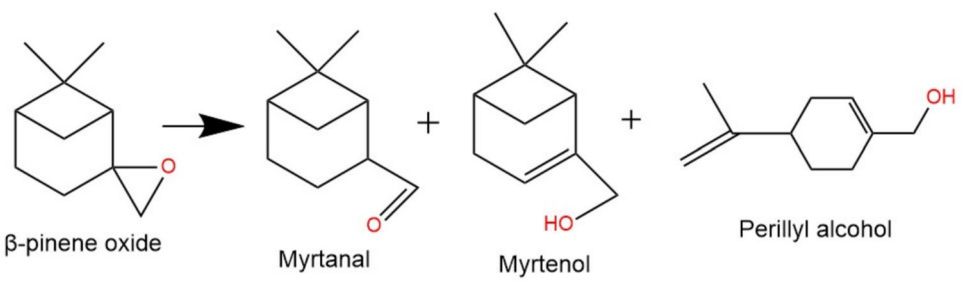


Figure 2 Main products from β-pinene epoxide isomerization.

(100% conversion, 85% selectivity) [24], $H_3PW_{12}O_{40}$ (94% conversion, 93% selectivity) [25], Ce/SiO_2 (98% conversion, 73% selectivity) [26], a hierarchical beta zeolite MZ-5 (92% conversion, 42% selectivity) [27], Fe-Beta-300 (100% conversion, 43% selectivity) [28]. For the isomerization of β-pinene epoxide different heterogeneous catalysts have been reported for the synthesis of myrtanal and perillyl alcohol (Table S2). Over 1.4/Fe-SBA-15 catalyst, 60% conversion and 100% selectivity toward myrtanal was reported (70 °C, 2 mg catalyst, 24 h and toluene as solvent) [9], with Mo/SBA-15 it was reported 99% conversion and 63% selectivity toward perillyl alcohol (80 °C, 10 mg catalyst, 1 h and hexane as solvent) [29]; in the case of Zr-beta zeolite, 99% conversion and 94% selectivity to myrtanal was reached (80 °C, 2 h, 50 mg catalyst, acetonitrile as solvent), the catalyst was recycled 8 times with no apparent loss of activity [30]. Sn-MCM-41 gave 66% selectivity to perillyl alcohol (DMSO as solvent, 70 °C, 10% wt.% catalyst, 24 h) [31]; over Fe supported on beta zeolite, perillyl alcohol was obtained with a selectivity up to 65% with 97% conversion with DMSO as solvent [32]. When the Zn-BTAlMg composite material was used, only myrtanal was obtained as product with a substrate conversion of 89% (dimethylcarbonate as solvent, 90 °C, 50 mg catalyst, 16 h); reusing tests showed that after the fourth reuse tests, β-pinene epoxide conversion decreased 11% [33].

The objective of this research was to evaluate the catalytic activity of catalysts synthesized using black sand; materials were characterized by TPD-NH_3, FTIR-Py, XRD, nitrogen isotherm, and SEM–EDX. In the isomerization of α- and β-pinene epoxides, the effect of solvent, temperature, amount of catalyst and time on the catalytic activity was evaluated. Finally, the heterogeneity of the synthesized catalysts was evaluated by leaching and reuse tests.

Experimental

Materials

Reactants were used as received. β-Pinene epoxide (96% w/w, synthesized according reported procedure [33] (Fig. S13) starting from (-)-β-pinene (Sigma Aldrich, 99% w/w)), α-pinene oxide (Sigma Aldrich, 97% w/w, Fig. S15, hexane (Honeywell, 98.63%), cyclohexane (Mallinckrodt, 100%), dioxane (Panreac, 99.5%), acetone (Supelco 99.8%), acetonitrile (Mallinckrodt 99.9%), ethyl acetate (Panreac 99.5%), heptane (Panreac 99%), tetrahydrofuran (J.T. Beaker 100%), toluene (J.T. Beaker 99.9%), sulfuric acid (Merck 95—97%), Fe_2O_3 (Alfa Aesar 98%), TiO_2 (Sigma Aldrich 99%).

Catalyst synthesis

The mining waste (black sand) supplied by Mineros S.A.S. (Colombia) was modified in the Applied Mineralogy and Bioprocesses Laboratory (GMAB) of the Universidad Nacional Medellín campus. The solid was sieved through 40 mesh screen and the passing solid was separated by low- and high-density magnetic separation and electrostatic separation. The obtained solid that corresponded to a treated black sand was named as TBS.

Treatment of black sand

The TBS solid was reduced in size using a Restch PM 100 corundum ball mill at 400 rpm for 2 h with a 3:1 mass ratio (balls: sample); the obtained solid was sieved using a 170 mesh screen and the solid was named IC.

Acid treatment with H_2SO_4

For the acid treatment, the IC sample was suspended in a 2 M H_2SO_4 aqueous solution with a 1:10 mass volume ratio of the solid to the acid solution in an autoclave at 100 °C for 4 h. Upon completion of the hydrothermal process, the suspension was vacuum filtered and washed with distilled water to pH 7. The solid was dried in an oven at 100 °C for 3 h and calcined at 400 °C for 2 h with a heating rate of 5 °C/min [34]. The obtained solid was named CAT_400.

Thermal treatment

For the thermal treatment, the solid IC was calcinated in a muffle at 800 °C for 3 h with a heating rate of 5 °C/min. The obtained solid was named CTT_800.

Characterization of catalysts

The iron and titanium content in CAT_400 and CTT_800 materials were measured by the means of atomic absorption spectroscopy using Agilent 200FS AA instrument, the samples prior analysis

was dissolved in HF/HNO_3-mixture. The textural properties were obtained by nitrogen physisorption isotherms at 77 K acquired using a Micromeritics ASAP 2020 PLUS instrument. Before analysis, the samples underwent pretreatment at 350 °C for 3 h under a high vacuum for degassing. Surface areas were determined utilizing the BET model, while the pore size distribution was calculated using the BJH model for the desorption isotherm, incorporating the Harkins and Jura correction. XRD analyses were performed on a Malvern-PANalytical Model Empyean 2012, with Pixel 3D detector and Cu source ($\lambda = 1.541874$ Å) at 45 kV and 40 mA; in the range of 10—80° (2θ) with a scanning step of 0.05°. The following patterns were used for the identification of the phases: ilmenite ($FeTiO_3$, ICSD 98–004–3466), hematite (Fe_2O_3, ICSD 98–017–4468), rutile (TiO_2, ICSD 98–003–3846), magnetite (Fe_3O_4, ICSD 98–009–6012), and pseudobrookite (Fe_2TiO_5, ICSD 98–002–4134). FTIR-Py analyses were performed by transmission on a Perkin Elmer Spectrum 65 FTIR Spectrometer by pretreating the sample with a flow of He (12.7 mL/min) up to 400 °C; pyridine was adsorbed at 30 °C for 60 min and then desorbed between 50 and 400 °C. The Raman spectra were taken using a confocal Lambram model spectrometer of high resolution with a CCD detector and a laser of 735 nm excitation wavelength. NH_3-TPD analyses were performed on a Micromeritics Autochem II 2290 instrument; the sample was treated at 350 °C for 30 min with He flow (50 mL/min), then ammonia was adsorbed at 50 °C and then desorbed by increasing the temperature at 10 °C/min up to 600 °C. The TCD signal was calibrated with ammonia mixtures of known composition, and the quantification of acidity (μmol NH_3/g) was performed using Eq. (1). X-ray photoelectron spectroscopy (XPS) measurements were performed on a SPECS brand X-ray photoelectron spectrometer (NAP-XPS) with a PHOIBOS 150 1D-DLD analyzer, using a monochromatic Al-Kα source (1486.7 eV, 13 kV). Samples were measured using a Flood Gun at 3 eV and 20 μA and the results were analyzed using Casa XPS software.

$$n_{Des} = 10^{-6} * \frac{\dot{V}_{He}}{V_m} * \frac{1}{\beta} * \int_{T_0}^{T_i} C_i dT \quad (1)$$

where n_{Des} are the moles of desorbed ammonia, $\dot{V}_{He}$ is the volumetric flow rate of carrier gas in mL/min, V_m is the molar volume in mL of one mole of gas at standard conditions (1 atm and 273.15 K), β is the heating rate in °C/min, and C_i is the concentration in ppm.

Catalytic activity

Isomerization of α- and β-pinene epoxide

Isomerization of α- and β-pinene epoxides were carried out in 2 mL vials covered with inert silicon septa and immersed in a Radley tech hotplate with magnetic stirring. In a typical experiment, the catalyst (25, 50, 75, and 100 mg) was mixed with 0. 25 mmol of the substrate in a 1 mL solvent (cyclohexane, heptane, hexane, toluene, tetrahydrofuran, ethyl acetate, acetone, and 1,4-dioxane) and the suspension was heated (60, 70, 80, and 90 °C) and stirred at 750 rpm for the selected time (0.5, 1, 1.5, 1.5, 2, and 2.5 h). The products were identified by gas chromatography using an Agilent 7890 A gas chromatograph with FID and Agilent 5975 C mass detector, using He as carrier gas. A DB-1 capillary column (30 m, 0.25 mm, 0.25 μm) and FID detector were used. The velocity and flow rate of the carrier gas was 30.5 cm/s and 2.2 mL/min, respectively. The oven temperature was 70 °C for 1 min and then increased to 90 °C (10 °C/min) for 0.5 min, then raised to 110 °C (10 °C/min) for 0.5 min, then to 130 °C (10 °C/min) for 0.5 min and finally up to 160 °C (15 °C/min) for 1 min. The injection volume was 1 μL in split mode (25:1) with injector temperature of 250 °C. Compound identification was performed using the NIST database5. Conversion and selectivity were calculated using Eqs. (2) and (3), respectively.

$$\%Conversion = \frac{\sum A_{pi}}{\sum A_{pi} + (A_R)} * 100 \quad (2)$$

$$\%Selectivity = \frac{(A_{Pi})}{\sum A_{pi}} * 100 \quad (3)$$

where A_{Pi} and A_R correspond to the area of product i and reactant, respectively, at the reaction time.

Leaching and reuse rests

To evaluate heterogeneity, the catalyst was separated from the reaction mixture after 12 min of reaction using a syringe filter with pore size of 0. 45 μm

Advantec brand syringe filter; an aliquot was taken and analyzed by GC–MS. The filtrate was left at the reaction conditions for further time and analyzed by GC–MS at 2, 4, 6, and 8 h. For reusing tests, the catalyst was separated by centrifugation at 3000 rpm for 10 min, washed with acetone three times, dried at 100 °C for 2 h and calcined at 400 °C (300 or 550 °C) for 2 h at 5 °C/min. The catalysts after the fifth reuse, calcined at 400 °C, and tested in the isomerization of α- and β-pinene epoxides were named CAT_400a and CAT_400b, respectively. Additional reuse tests were performed with the catalyst treated with sulfuric acid after its first use, using the procedure described for the IC sample.

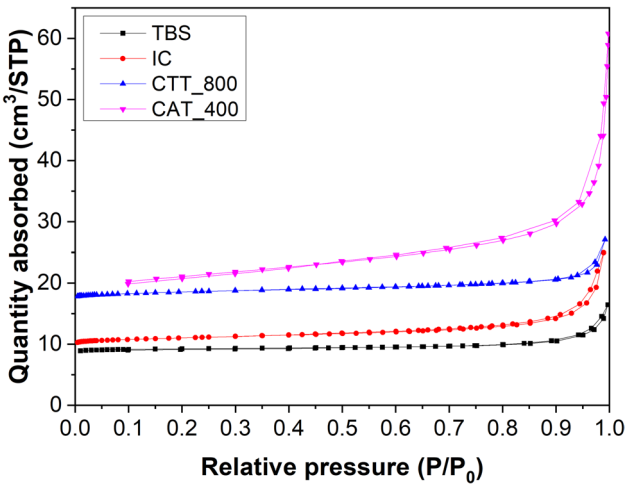


Figure 3 Nitrogen adsorption–desorption isotherm of TBS, IC, CTT_800 and CAT_400 materials.

Results and discussions

Catalyst characterization

Textural properties

Figure 3 and Table 1 show the textural properties obtained by nitrogen adsorption–desorption of the materials obtained from black sand treatment; these analyses were performed for identifying characteristics of the materials as porosity and surface area that could favor the availability of active sites for the reaction. TBS, IC and CTT_800 materials show a type I(b) isotherm (according to IUPAC classification) [35], the isotherms of these samples are characteristic of microporous solids that have relatively small external surfaces, and pore size distributions < 2.5 nm. The BET surface area for TBS, IC and CTT_800 were 3.89, 5.13 and 4.23 m^2/g, respectively. Additionally, pore diameters of 1.81, 2.07 and 1.91 nm were found for TBS, IC and CTT_800 materials, respectively. For the CAT_400 material, a type II isotherm with an H3 hysteresis (according to the IUPAC classification) was observed [35]; the BET surface area was 18.18 m^2/g with a pore diameter of 3.42 nm, the higher porosity and surface area of CAT_400 is attributed to the hydrothermal treatment with H_2SO_4. It was found that the treatment with sulfuric acid and later thermal treatment increased pore size, surface area, and pore volume. As the molecular size of α-pinene epoxide (0.64 nm) [36] and β-pinene epoxide (0.70 nm) [37] are lower than the pores of CTT_800 (1.91 nm) and CAT_400 (3.42 nm), the molecules can pass through the pores of the catalysts for being transformed; furthermore, the reaction is facilitated with the largest pore size catalyst.

Table 1 Metal content and textural properties of TBS, IC, CTT_800 and CAT_400 materials

Sample	S_{BET} (m^2/g)	V_p (cm^3/g)	D_p (nm)	Metal content (% w/w)a		AS (mmol/m^2)[b]
				Ti	Fe	
TBS	3.89	0.01	1.81	ND	ND	ND
IC	5.13	0.02	2.07	ND	ND	ND
CTT_800	4.23	0.01	1.91	9.24	4.41	0.50
CAT_400	18.18	0.06	3.42	9.51	7.87	0.14

V_p: pore volume, D_p: pore diameter, AS: active sites concentration. [a]Evaluated by atomic absorption. [b]Assuming that Fe^{3+} and Ti^{4+} are the active sites; $AS = (x_{Ti^{+4}}/mw_{Ti} + x_{Fe^{+3}}/mw_{Fe})/S_{BET}$, $x_{Ti^{+4}}$ and $x_{Fe^{+3}}$ are the mass fraction of Ti^{4+} and Fe^{3+}, respectively, that were calculated using the metal content evaluated by atomic absorption and the concentration of Ti^{4+} and Fe^{3+}obtained by XPS, mw_{Ti} and mw_{Fe} are the molecular weight of Ti and Fe, respectively. ND: not determined

Table 2 Phase composition (%) of the obtained solids

Sample	Ilmenite	Hematite	Rutile	Magnetite	Pseudobrookite
TBS	58.5	30.0	11.5	0	0
IC	51.5	35.7	12.8	0	0
CTT_800	14.3	44.5	30.4	9.3	1.5
CAT_400	29.9	52.7	17.4	0	0

Table 1 shows that titanium content is similar in CTT_800 and CAT_400; however, iron content is higher in CAT_400. The active site concentration was calculated with the surface area, the total content of Fe and Ti, and the content of Fe^{3+} and Ti^{4+} that were determined by XPS (Sect. XPS analysis). As the surface area of CAT_400 is higher, the density of active sites is lower than in the case of CTT_800.

XDR analysis

Figure S2 of the Supporting Information shows the diffractograms corresponding to the different materials (IC, TBS, CATT_800, CAT_400). Using the high score software, different mineralogical phases were identified in the solids. All the materials contain ilmenite, hematite, and rutile phases; furthermore, CTT_800 also present magnetite and pseudobrookite phases. Table 2 shows the semi-quantitative analysis of the phases calculated by Rietveld refinement of the diffractograms. It is observed that ilmenite is transformed into hematite and rutile mainly using milling processes and hydrothermal treatment with H_2SO_4. Additionally, the material that was obtained by calcination at 800 °C also presents magnetite and pseudobrookite phases. It has been reported that by milling processes, ilmenite is transformed into hematite and rutile due to the breaking of chemical bonds [38], according to Eq. (4); for this reason, there is a decrease in the amount of the ilmenite phase after milling. Ilmenite oxidizes in the presence of air and decomposes into hematite and rutile at a temperature below 800 °C, and pseudobrookite above 850 °C [39].

$$2FeTiO_3 + 0.5O_2 \rightarrow 2TiO_2 + Fe_2O_3 \quad (4)$$

The transformation of ilmenite into rutile and hematite after calcination of the solid obtained by hydrothermal reaction of the black sand after milling with a 2 M solution of sulfuric acid can be explained in four stages: (i) digestion of ilmenite in the presence of sulfuric acid that produces iron sulfate and titanyl sulfate, Eq. (5) [3]; (ii) hydrolysis of titanyl sulfate into hydrated titanium dioxide, Eq. (6) and iron sulfate into iron hydroxide, Eq. (7) [3, 40]; (iii) removal of sulfuric acid by washing with distilled water, which was confirmed by FTIR analysis of the solid washed with water at 85 °C and at room temperature (Figure S1); (iv) calcination of the solid that removes water of hydration of titanium dioxide, Eq. (8), and transforms iron hydroxide into hematite, Eq. (9) [3, 41].

$$FeTiO_3 + 2H_2SO_4 \rightarrow FeSO_4 + TiOSO_4 + 2H_2O \quad (5)$$

$$TiOSO_4 + (n + 1)H_2O \rightarrow TiO_2nH_2O + H_2SO_4 \quad (6)$$

$$FeSO_4 + 2H_2O \rightarrow Fe(OH)_2 + H_2SO_4 \quad (7)$$

$$TiO_2nH_2O \rightarrow TiO_2 + nH_2O \quad (8)$$

$$2Fe(OH)_2 \rightarrow Fe_2O_3 + H_2O \quad (9)$$

XPS analysis

XPS was used to examine the elemental composition and oxidation states of catalysts synthesized from ilmenite. The XPS spectra shown in Figs. 4a and 5a confirm the presence of Fe, Ti, and O in CAT_400 and CTT_800 catalysts; no S signals were identified in Fig. 4a. Figures 4b and 5b show the high-resolution spectrum of Fe 2p; after deconvolution of the spectrum four peaks were determined. The signals at 711.2 eV and 724.7 eV correspond to Fe $2p_{3/2}$ and Fe $2p_{1/2}$, respectively which are attributed to the Fe^{+2} oxidation state and the energies of 712.9 eV and 726.5 eV correspond to Fe $2p_{3/2}$ and Fe $2p_{1/2}$, respectively, that are attributed to Fe^{+3} [42–45]. The presence of Fe^{+2} and Fe^{+3} is associated to $FeTiO_3$ and Fe_2O_3 that were identified by XRD and Raman analysis. The content of Fe^{3+}, determined by XPS, was 69% and 86% for CAT_400

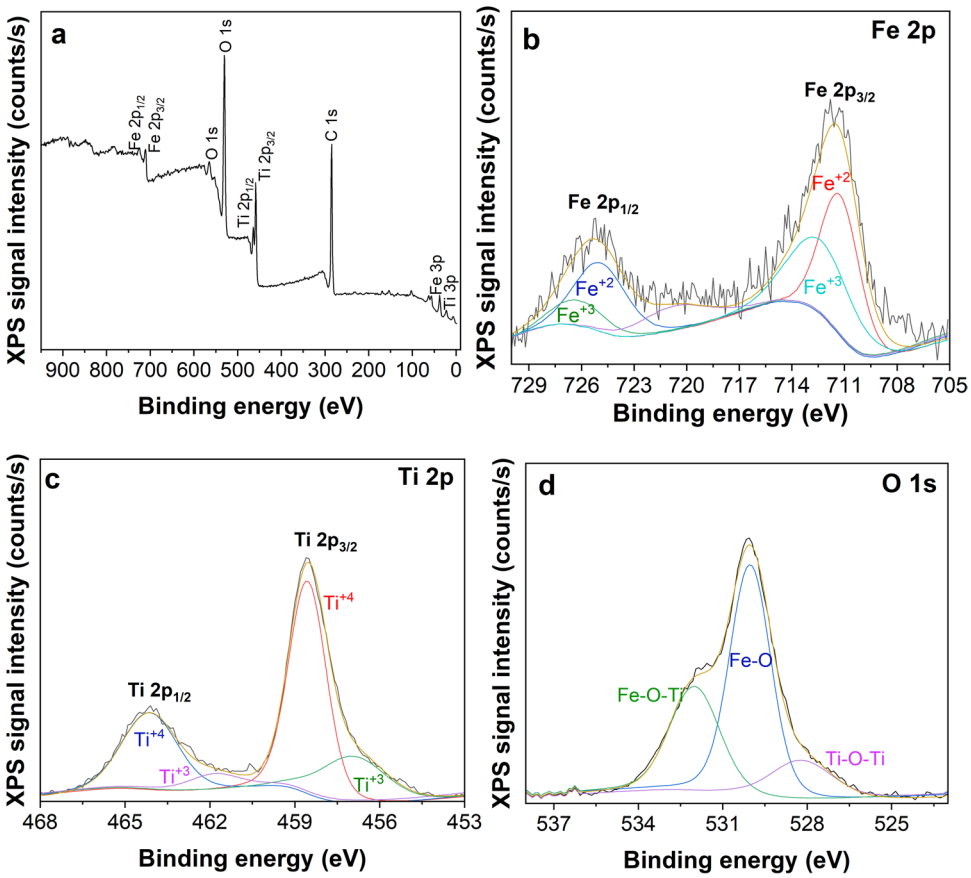


Figure 4 XPS spectra of CAT_400 (**a**) and the corresponding high-resolution spectra of Fe 2p (**b**), Ti 2p (**c**), and O 1 s (**d**) elements.

and CTT_800, respectively. Figures 4c and 5c show four peaks for the high-resolution of Ti 2p spectrum; the peaks at 458.5 eV and 464.3 eV correspond to Ti $2p_{3/2}$ and Ti $2p_{1/2}$, respectively, which are attributed to the Ti^{+4} oxidation state of the rutile phase and the peaks at 457.4 eV and 463.1 eV correspond to Ti $2p_{3/2}$ and Ti $2p_{1/2}$ respectively, and are attributed to Ti^{+3} [42, 43, 45]. The content of Ti^{4+}, determined by XPS, was 77% and 74% for CAT_400 and CTT_800, respectively Therefore, ilmenite has the co-existence of multivalent oxidation states, such as Ti^{+4}/Ti^{+3} and Fe^{+3}/Fe^{+2}, where the charge neutralization can be acquired through the O atoms [42]. The high-resolution of O 1 s spectrum in Figs. 4d and 5d shows three peaks at 529.3, 530.0 eV, 531.6 eV corresponding to the O element in TiO_2, Fe–O and $FeTiO_3$, respectively [46].

Raman analysis

Figure 6 shows the Raman spectra of the synthesized materials. The peaks at 214 cm^{-1}, 282 cm^{-1}, and 409 cm^{-1} are characteristic of hematite [12, 45]; the peak at 147 cm^{-1} is characteristic of rutile [47]. The peaks at 223 cm^{-1} and 675 cm^{-1} are characteristic of ilmenite [48]. Moreover, in the CTT_800 solid, different peaks are observed; peaks at 364 cm^{-1}, 540 cm^{-1}, and 675 cm^{-1} are characteristic to magnetite [49]. The Raman analysis data agree with the conclusion on the crystallographic phases determined by XRD analysis, that showed ilmenite transformation into hematite and rutile after milling and hydrothermal acid treatment. The modifications performed on the mining residue increased the hematite and rutile content; both hematite and rulite were reported as catalysts for the rearrangement of α-pinene epoxide [16].

SEM–EDX analysis

Figure 7a and b shows the surface morphology of the mining residue before and after ball milling, respectively; the surface modifications, structural defects, and fractures are due to impact and shear forces induced by mechanical wear [50]. The predominant crystallographic phase in the mining

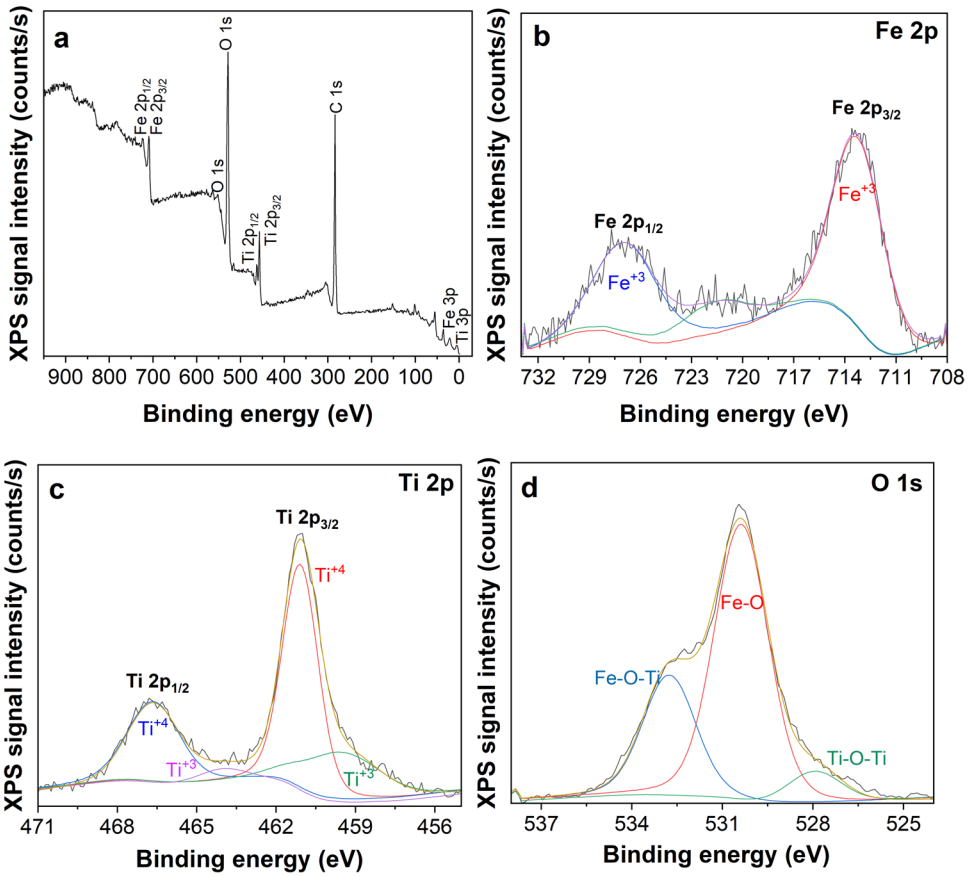


Figure 5 XPS spectra of CTT_800 (**a**) and the corresponding high-resolution spectra of Fe 2p (**b**), Ti 2p (**c**), and O 1 s (**d**) elements.

residue is ilmenite; in the literature it has been shown that the grinding process reduces the crystal size and increases the surface area [50]. Figure 7c and d shows the solids obtained by heat treatment and hydrothermal reaction with H_2SO_4 in which particle size < 10 μm with undefined morphology is observed. The result of the EDX analysis presented in Table 3 indicates that the predominant elements are Fe, Ti, and O; in addition, traces of Mn, Si, V, Ca, and Cu are evidenced in TBS, IC and CTT_800 solids; but are absent in the solid CAT_400 what was attributed to leaching during processing with H_2SO_4. This result is in good agreement with XRD analysis. Figure S3–S6 of the Supporting Information show the mapping analysis of the elements presented in the samples; from the data a uniform distribution of all the elements is evident.

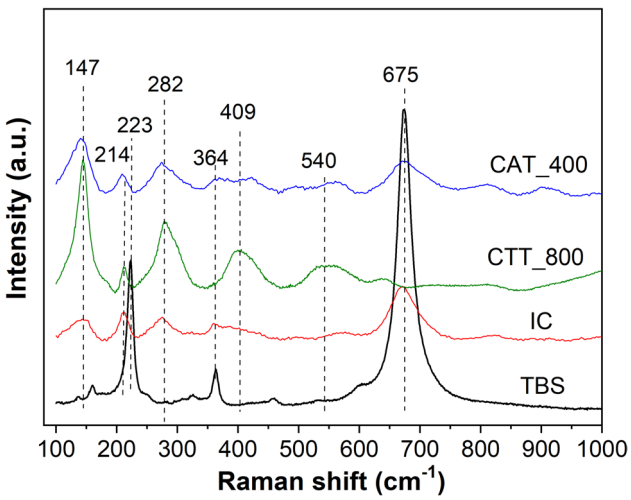


Figure 6 Raman spectra of TBS, IC, CTT_800, and CAT_400 materials.

Acidity

NH_3 -TPD analysis of the materials (TBS, IC, CAT_400, and CTT_800) is shown in Fig S6 and Table 4 that shows the distribution of the acidity strengths and the amount of $\mu mol_{NH3} \cdot g^{-1}$. It has been reported that hematite (Fe_2O_3) presents medium and strong acid sites [51], and rutile (TiO_2) presents low, medium, and

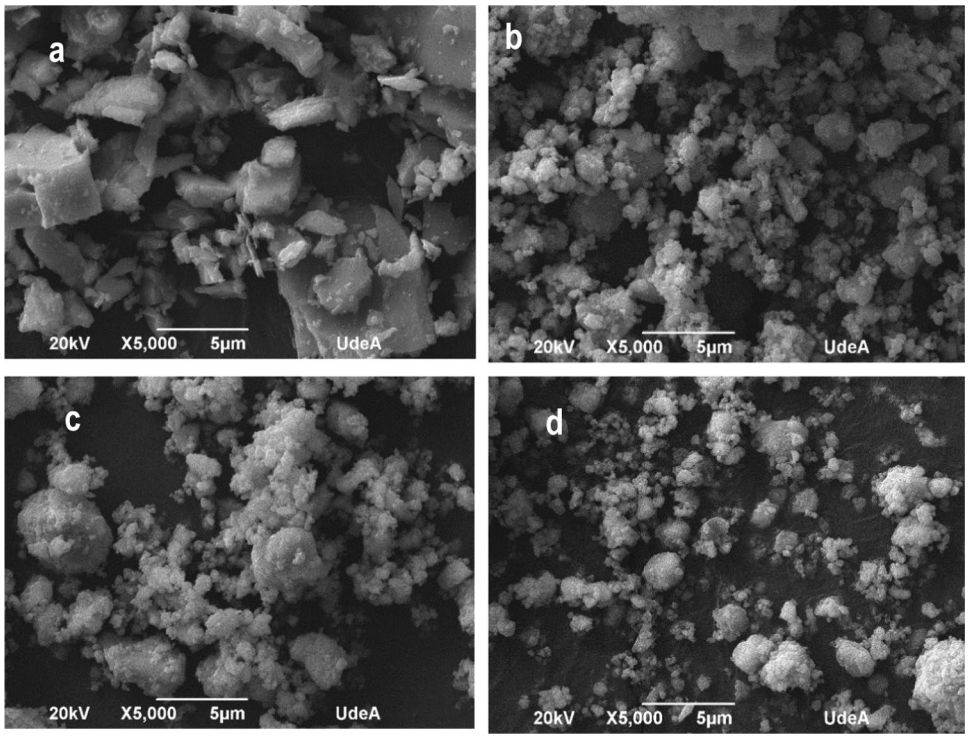


Figure 7 SEM–EDX images of TBS (**a**), IC (**b**), CTT_800 (**c**), and CAT_400 (**d**).

Table 3 SEM–EDX analysis of catalysts synthesized from ilmenite

	Sample (wt %)			
Element	TBS	IC	CTT_800	CAT_400
Fe	41.83 ± 0.3	45.92 ± 0.39	43.69 ± 0.45	42.69 ± 0.78
Ti	30.3 ± 0.23	28.87 ± 0.26	28.47 ± 0.31	40.26 ± 0.73
O	20.97 ± 0.51	20.5 ± 0.62	22.5 ± 0.73	8.33 ± 1.59
Mn	2.59 ± 0.07	1.88 ± 0.08	1.69 ± 0.1	2.2 ± 0.15
Si	2.05 ± 0.05	0.73 ± 0.05	0.86 ± 0.07	0
Al	1.64 ± 0.05	0.81 ± 0.06	1.62 ± 0.08	6.52 ± 0.18
V	0.22 ± 0.05	0.25 ± 0.08	0.31 ± 0.09	0
Ca	0.23 ± 0.07	0.22 ± 0.04	0.17 ± 0.05	0
Cu	0.16 ± 0.03	0.76 ± 0.12	0.71 ± 0.14	0

Table 4 Quantification of acid sites by NH_3-TPD ($\mu mol_{NH3}/g$)*

Sample	Low acidity (100–220 °C)	Medium acidity (220–400 °C)	Strong acidity (400–600 °C)	Total
TBS	0	130	37	167
IC	121	0	93	214
CTT_800	0	316	0	316
CAT_400	171	0	193	364

*The type of acidity was classified according to reference [53]

strong acid sites [52]. In the solids synthesized by heat treatment and hydrothermal reaction with H_2SO_4, the hematite and rutile content increased, causing a rise in the strong acid sites, especially in the catalyst synthesized with H_2SO_4 (CAT_400) that contains higher amount of hematite.

An important characteristic of catalysts used on the monoterpene epoxides isomerization is their acidity [54]. It has been reported that the isomerization of α-pinene epoxide and the selectivity of the products depend on the type of acid sites; campholenic aldehyde and *trans*-carveol formation is promoted, respectively, when Lewis and Brønsted acid sites are present [30]. In addition, high yields of myrtanal are obtained by the isomerization of β-pinene epoxide in the presence of Lewis acid sites [9]. Figure 8 shows the acid sites of the catalysts synthesized from black sand, desorbed pyridine peaks at 1448 cm^{-1} and 1615 cm^{-1} are characteristic of Lewis acid sites and the peak at 1491 cm^{-1} is characteristic of mixture of Lewis and Brönsted acid sites [55, 56]. No Brønsted acid sites were identified by py-FTIR in the analyzed materials; neither the peak at 1638 nor at 1545 cm^{-1} [57] were detected. The vibrational modes ν(CCN)

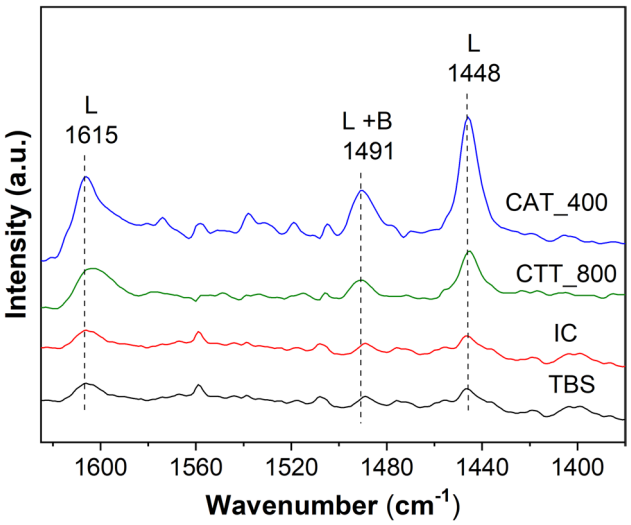


Figure 8 FTIR of pyridine desorbed at 50 ºC for TBS, IC, CTT_800, and CAT_400. Lewis (L) and Brønsted (B) acid sites.

(v_{8a}, v_{8b}, v_{19a}, and v_{19b}) appear in the frequency range between 1650 and 1400 cm^{-1}. The vibrational modes v_{8a} and v_{19a} correspond to coordinated pyridine with Lewis sites desorbing in the region 1633—1600 cm^{-1} and 1460–1445 cm^{-1}, respectively [58, 59]. In Fig. 8, the peak at 1491 cm^{-1} should be related only to Lewis acid sites, because no Brønsted sites were identified. Lewis acid sites are attributed to the presence of Fe^{+3} from hematite (Fe_2O_3) phase [36, 39]; for rutile (TiO_2) characteristic signals of Lewis acid site at 1445, 1489, and 1605 cm^{-1} have been reported [60]. Figure S8 of the Supporting Information shows that after 300 °C the peaks related to Lewis acid sites still appears in CAT_400, IC, and TBS materials indicating the presence of strong acid sites [61], which agrees with the results obtained by NH_3 -TPD.

Catalytic tests

Effect of solvent on the isomerization of α- and β-pinene epoxide

The isomerization of α- and β-pinene epoxides was evaluated with various solvents and the synthesized catalysts (CTT_800 and CAT_400) because it has been reported that the selectivity of the isomerization of monoterpene epoxides depends on the solvent polarity [9, 15, 35]. First, the effect of the solvent (Table 5) was evaluated on α-pinene epoxide conversion and products selectivity, using CTT_800 catalyst. It was found that in the presence of toluene, ethyl acetate or tetrahydrofuran, no substrate conversion was observed; however, α-pinene epoxide conversion was around 10% when cyclohexane, hexane, or heptane were used as solvents and campholenic aldehyde selectivity was around 80%. When CAT_400 was used as catalyst with cyclohexane as solvent (0.25 mmol of α-pinene epoxide, 70 °C, 50 mg of catalyst), α-pinene epoxide conversion and campholenic aldehyde selectivity were 28% and 65%, respectively. The higher activity of CAT_400 could be related to its better textural properties that allow a higher availability of active sites for the reaction. The observed effect of the solvent on campholenic aldehyde selectivity agrees with reports of non-polar solvents that favor campholenic aldehyde production [62]; although, it has also reported that low-basic non-polar solvents favor campholenic aldehyde production [63].

When CTT_800 was used as catalyst for the isomerization of β-pinene epoxide with the same solvents used for the isomerization of α-pinene epoxide, no substrate conversion was observed. The effect of solvent on β-pinene epoxide isomerization over CAT_400 was evaluated and the results are shown in Table 6.

Table 5 Effect of the solvent on α-pinene epoxide conversion and product selectivity over CTT_800

Solvent	Polarity	Dielectric constant [11]	X (%)	Selectivity (%)					
				Ac	CV	tP	IC	pC	Ot
Heptane	No- polar	1.99	8	78	7	5	3	1	6
Hexane	No- polar	1.99	10	81	6	4	3	2	4
Cyclohexane	No- polar	2.02	10	80	7	4	3	2	4
Dioxane	Polar aprotic	2.25	0	0	0	0	0	0	0
Ethyl acetate	Polar aprotic	6.02	0	0	0	0	0	0	0
Tetrahydrofuran	Polar aprotic	7.52	0	0	0	0	0	0	0

Reaction conditions: 0.25 mmol α-pinene epoxide, 50 mg CTT_800, 1 mL solvent, 750 rpm, 2 h, 70 °C. X: Conversion of α-pinene epoxide Ac: campholenic aldehyde, CV: *cis*-carveol, tP: *trans*-pinocarveol, IC: isocamphorone, pC: *p*-cymene, Ot: others

Table 6 Effect of the solvent on β-pinene epoxide conversion and product selectivity over CAT_400

Solvent	Polarity	Dielectric constant [11]	X (%)	Selectivity (%)			
				My	Mt	Ap	Other
1,4-Dioxane	Polar aprotic	2.25	30	96	0	0	4
Ethyl acetate	Polar aprotic	6.02	42	84	0	0	16
Tetrahydrofuran	Polar aprotic	7.52	12	78	0	0	22
Acetone	Polar aprotic	20.7	58	67	11	9	13
Hexane	No-polar	1.99	5	28	10	37	25
Cyclohexane	No-polar	2.02	17	39	19	39	4
Toluene	No-polar	2.38	0	0	0	0	0

Reaction conditions: 0.25 mmol β-pinene epoxide, 50 mg CAT_400, 1 mL solvent, 750 rpm, 2 h, 70 °C. X: Conversion of β-pinene epoxide, My: myrtanal, Mt: myrtenol, Ap: perillyl alcohol

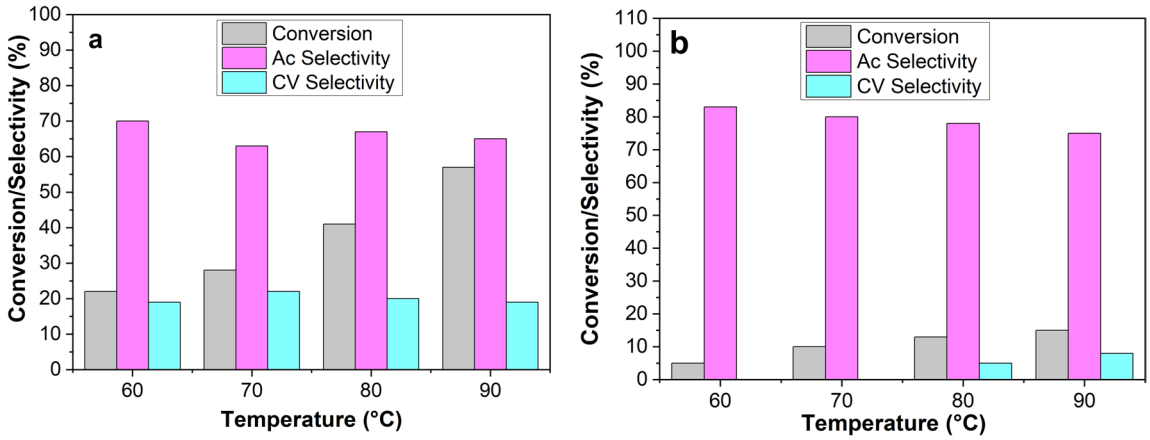


Figure 9 Effect of temperature on isomerization of α-pinene epoxide over CAT_400 (**a**) and CTT_800 (**b**) catalysts. Reaction conditions: 0.25 mmol α-pinene epoxide, 1 mL cyclohexane, 2 h, 750 rpm, 50 mg catalyst. AC: campholenic aldehyde, CV: *cis*-carveol.

It was found that dioxane was a good solvent for myrtanal production (up to 96%), and that for polar solvents, the myrtanal selectivity decreased when the dielectric constant increased. The following order of conversion was found: acetone > ethyl acetate > dioxane > cyclohexane > tetrahydrofuran > hexane. Although acetonitrile is a polar solvent, when it was used as solvent, no reaction was detected, probably because the solvent is adsorbed on the active sites, avoiding the adsorption of the reagent. The affinity of the catalyst for this solvent could be related to the available electrons of the solvent. It has been reported that myrtanal formation is favored with apolar solvents [36]; over Fe/MCM-41 the best β-pinene epoxide conversion and myrtanal selectivity (up to 90%) was achieved with acetonitrile [12] and over a Colombian natural zeolite, in the presence of dioxane no β-pinene epoxide conversion was found [36]. The differences on solvent effect on myrtanal selectivity could be related to the chemical species that are formed in the catalytic systems and the stabilization and rearrangement of the intermediate carbocation [11].

Effect of temperature on the isomerization of α- and β-pinene epoxide.

Figure 9 shows that α-pinene epoxide conversion increases with temperature over CTT_800 and CAT_400 from 60 to 90 °C; however, temperature effect is higher over CAT_400. Furthermore, campholenic aldehyde selectivity is approximately constant and higher in the case of CTT_800. Also, an increase of conversion and a similar campholenic aldehyde was reported with temperature increase over zirconium phosphate catalyst [64]. Similarly, Fig. 10 shows that over CAT_400, β-pinene epoxide conversion increases with temperature and myrtanal selectivity

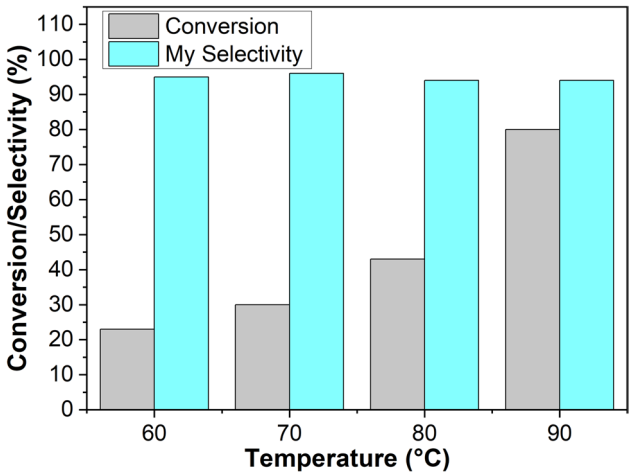


Figure 10 Effect of temperature on isomerization of β-pinene epoxide over CAT_400. Reaction conditions: 0.25 mmol β-pinene epoxide, 50 mg catalyst, 1 mL solvent, 750 rpm, 2 h. My: myrtanal.

does not change. Similar results were reported over Sn-Y-12 [65] and over a Colombian natural zeolite [36].

Effect of catalyst amount

Different amounts of catalyst were tested in the isomerization of α- and β-pinene epoxides using cyclohexane and dioxane as solvents, respectively. For the isomerization of α-pinene epoxide (Fig. 11.) with a catalyst concentration (CAT_400) of 25 mg/mL, a conversion of 30% was obtained and selectivity to campholenic aldehyde of 66% and 17% to *cis*-carveol. When the catalyst concentration increased to 100 mg/mL, the conversion was 95%, and the selectivity to campholenic aldehyde and *cis*-carveol did not have a significant change. On the contrary, when the concentration of CTT_800 increased from 25 mg/mL to 100 mg/mL, conversion enhanced from 6 to 27%, and the selectivity to campholenic aldehyde was between 70 and 80%.

In the rearrangement of β-pinene epoxide over CAT_400 (Fig. 12), increasing catalyst concentration from 25 to 75 mg/mL, caused an enhancement in conversion from 41 to 95% without change of myrtanal selectivity (> 93%). It has been reported that using a Colombian natural zeolite, the conversion increased from 36 to 97% and myrtanal selectivity was approximately constant when catalyst concentration increased from 2 to 25 mg/mL [36].

Effect of time

Figure S9 and Figure S10 show that the conversion of α-pinene epoxide and β-pinene epoxide over CAT_400, respectively, increased with time and that products selectivity did not change. For α-pinene epoxide at 2.5 h, conversion was 96% and campholenic aldehyde selectivity was 64%. In the case of β-pinene epoxide, at 2.5, the conversion was 98% and myrtanal selectivity was 92%.

Blank reaction in the isomerization of α- and β-pinene epoxides

Tables 7 and 8 show the results of the blank reactions evaluated under the best reaction conditions in the isomerization of β-pinene epoxide and α-pinene epoxide, respectively. For the isomerization of both epoxides there was not conversion in the absence of catalyst. Catalytic tests were performed with commercial hematite (Fe_2O_3) and rutile (TiO_2) and a black sand enrichment with ilmenite, using the same amount contained in the CAT_400 catalyst of each of the phases according to Rietveld refinement of the diffractograms; catalytic tests were also carried out with the same used amount of the CAT_400 catalyst. In the isomerization of α-pinene epoxide with commercial hematite (Fe_2O_3) a conversion of 47% and selectivity toward campholenic aldehyde of 65% was obtained and with commercial rutile (TiO_2) a conversion of 98% and selectivity to campholenic aldehyde of 60% was obtained; furthermore, with black sand enrichment with ilmenite, a low conversion was observed with a high selectivity to campholenic aldehyde. In the isomerization of β-pinene epoxide with commercial hematite (Fe_2O_3) a conversion and selectivity to myrtanal of 47% and 90% were observed, respectively; with commercial rutile a conversion and selectivity to myrtanal of 92% and 86% were reached; however, with black sand enrichment with ilmenite, no reaction was detected. It has been reported [9] that the isomerization of α-pinene epoxide over hematite is promoted by the empty d orbitals of Fe^{+3}.

In addition, a mechanical mixture of hematite and commercial rutile with similar composition to the

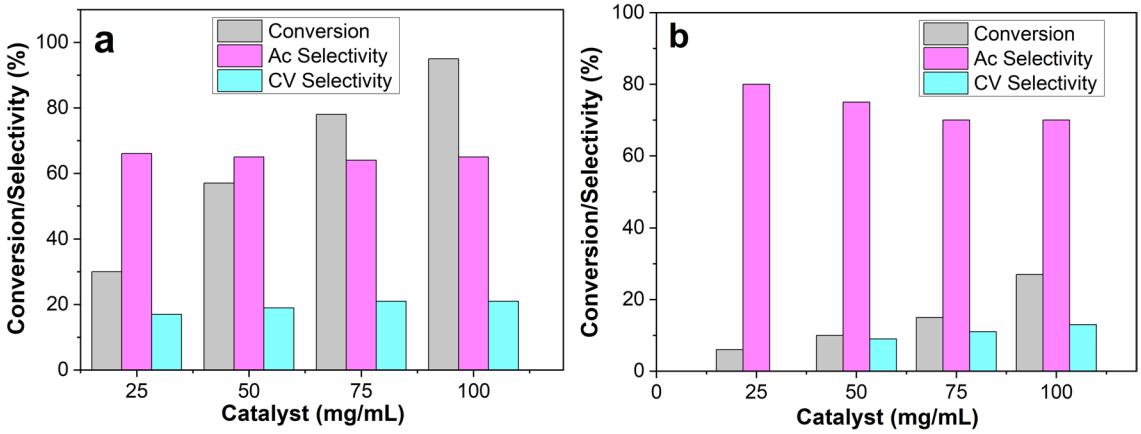


Figure 11 Effect of catalyst concentration on the isomerization of α-pinene epoxide over CAT_400 (**a**) and CTT_800 (**b**) catalyst. Reaction conditions: 0.25 mmol of α-pinene epoxide, 1 mL cyclohexane, 2 h, 750 rpm, 90 °C, Ac: campholenic aldehyde, CV: *cis*-carveol.

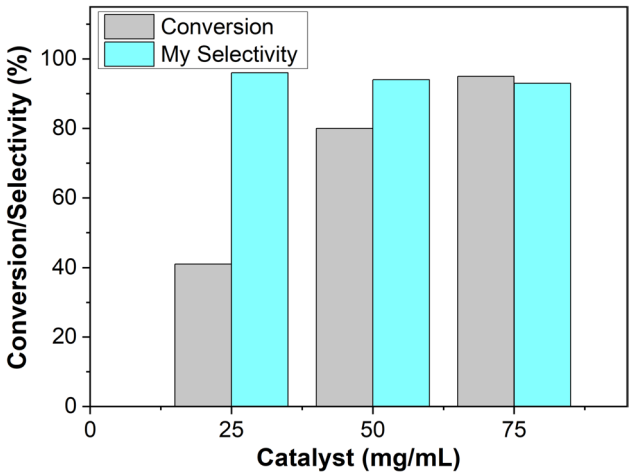


Figure 12 Effect of catalyst concentration on the isomerization of β-pinene epoxide over CAT_400. Reaction conditions: 0.25 mmol β-pinene epoxide, 1 mL dioxane, 2 h, 750 rpm and 90 °C. My: myrtanal.

synthesized CAT_400 catalyst was performed where a conversion of α- and β-pinene epoxides of 54 and 64% was obtained, respectively. Furthermore, with the IC material, a conversion of α- and β-pinene epoxides of 4% and 2%, respectively, was obtained; probably the acidity of the mining waste is not enough for epoxide isomerization. From blank reactions it is possible to conclude that it is not enough that the catalyst contains Ti and Fe for promoting the reaction; it is necessary that the material contains the appropriate phases. Hematite and rutile are active phases for the isomerization of α- and β-pinene epoxides; TiO_2 favored epoxide conversion and Fe_2O_3 aldehyde selectivity.

Table 7 Blank reactions for the isomerization of β-pinene epoxide

Catalyst (mg)	X (%)	Selectivity (%)			
		My	Mt	Ap	Other
None	0	0	0	0	4
IC (75)	4	100	0	0	16
TiO_2 (78.4)[a]	92	86	11	3	22
TiO_2 (15.6)[b]	41	85	11	4	13
Fe_2O_3 (75)[a]	38	98	3	0	25
Fe_2O_3 (39.3)[b]	47	90	1	8	4
Fe_2O_3 (39.7) and TiO_2 (13.3)[c]	64	93	5	2	0
CAT_400 (75)	98	92	0	8	0
$FeTiO_3$ (100)	0	0	0	0	0

Reaction conditions: 0.25 mmol of β-pinene epoxide, 1 mL cyclohexane, 2 h, 750 rpm, 90 °C. X: Conversion of β-pinene epoxide, My: myrtanal, Mt: myrtenol. [a]The same amount of CAT_400 catalyst used in the catalytic tests. [b]The same amount contained in the CAT_400 catalyst according to Rietveld refinement of the diffractograms. [c]Mechanical mixture

Higher conversion was observed with the catalyst synthesized with the mining residue compared to the mechanical mixture of hematite and rutile, while the selectivity of the products is similar. This could indicate that the reaction is not only promoted by the presence of the two phases, but that the proximity between the phases in the CAT_400 catalyst is important for the transformation of the monoterpene isomer; as it was verified by Raman and DRX analysis, CAT_400 presented higher hematite and rutile phases content that

Table 8 Blank reactions for the isomerization the α-pinene epoxide

Catalyst (mg)	X (%)	Selectivity (%)					
		Ac	CV	tP	IC	pC	tC	Ot
None	0	0	0	0	0	0	0	0
IC (100)	2	100	0	0	0	0	0	0
TiO_2 (100)[a]	98	60	6	26	6	0	1	1
TiO_2 (19.2)[b]	40	41	4	47	8	0	0	0
Fe_2O_3 (100)[a]	43	65	20	3	3	3	5	2
Fe_2O_3 (52.6)[b]	15	64	20	6	4	2	3	1
Fe_2O_3 (52.6) and TiO_2 (19)[c]	54	53	10	28	6	1	2	0
CAT_400 (100)	96	65	21	5	3	1	3	2
$FeTiO_3$ (100)	8	81	7	8	0	4	0	0

Reaction conditions: 0.25 mmol of α-pinene epoxide, 1 mL cyclohexane, 2 h, 750 rpm, 90 °C. Ac: campholenic aldehyde, CV: *cis*-carveol, tP: *trans*-pinocarveol, IC: isocamphone, pC: *p*-cymene. [a]The same amount of CAT_400 catalyst used in the catalytic tests. [b]The same amount contained in the CAT_400 catalyst according to Rietveld refinement of the diffractograms. [c]Mechanical mixture

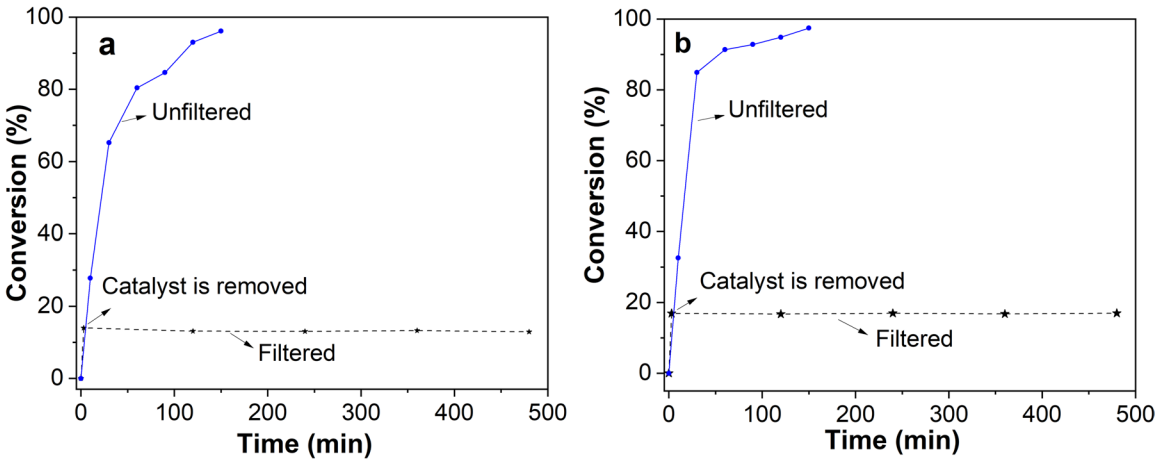


Figure 13 Leaching test of CAT_400 in the isomerization of α-pinene epoxide (**a**) and β-pinene epoxide (**b**). Reaction conditions: 100 mg catalyst, 90 °C, 0.25 mmol pinene epoxide, 750 rpm.

the black sand. It has been reported that Fe^{+3}, instead of Fe^{+2}, are the active species in the isomerization of α-pinene epoxide toward campholenic aldehyde [66]; furthermore, it has been found that the presence of Ti^{+4} in heterogeneous catalysts and non-polar solvents favored campholenic aldehyde production [17]. The transformation of the tested monoterpenic epoxides toward aldehydes can be attributed to the presence of Fe^{+3} and Ti^{+4} in the hematite and rutile phases, respectively, that are contained in the evaluated catalyst.

Reuse and leaching tests of catalysts

No leaching was detected neither in the isomerization of α-pinene epoxide nor in β-pinene epoxide isomerization using the catalyst synthesized by hydrothermal treatment with H_2SO_4, as shown in Fig. 13. The catalyst was reused five times in the two reactions (Figs. 14 and 15), treating the catalyst at 400 °C before each reuse; in the isomerization of α-pinene epoxide the conversion decreased 56%; for the isomerization of β-pinene epoxide the conversion decreased 52% with respect to the fresh catalyst. No changes in selectivity were observed for the

tested catalysts. As substrate conversion decreased after catalyst reuse, additional catalyst treatments before reusing tests were evaluated. The catalyst was calcined at 300 or 550 °C, or treated again with sulfuric acid. Figure 16 shows that an increase in calcination temperature caused a decrease of substrate conversion, specially at temperatures higher than 550 °C which could be related to formation of other phases that do not favor monoterpene epoxide isomerization. The solid treated with acid showed a similar behavior than the catalyst calcined at 400 °C, which is a simplest procedure. In conclusion, the best catalyst activation is the treatment at 300 °C.

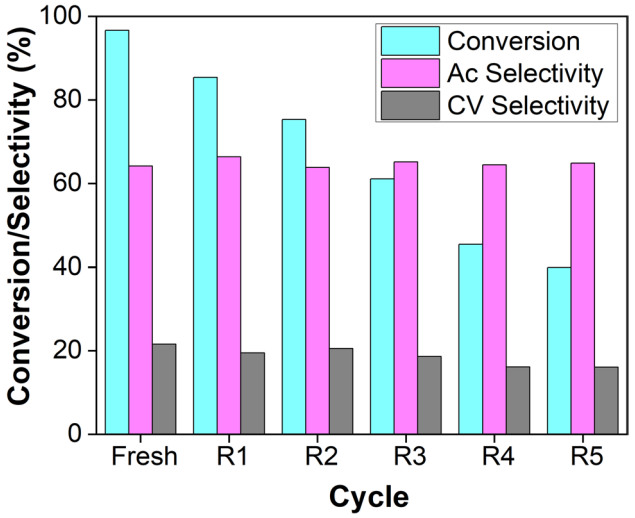


Figure 14 Reuse of CAT_400 catalyst in the isomerization of α-pinene epoxide. Reaction conditions: 100 mg catalyst, 90 °C, 0.25 mmol α-pinene epoxide, 750 rpm. The catalyst before reuses (Rx, with x the number of reuses) was washed with acetone and calcined at 400 °C (5 °C/min) for 2 h.

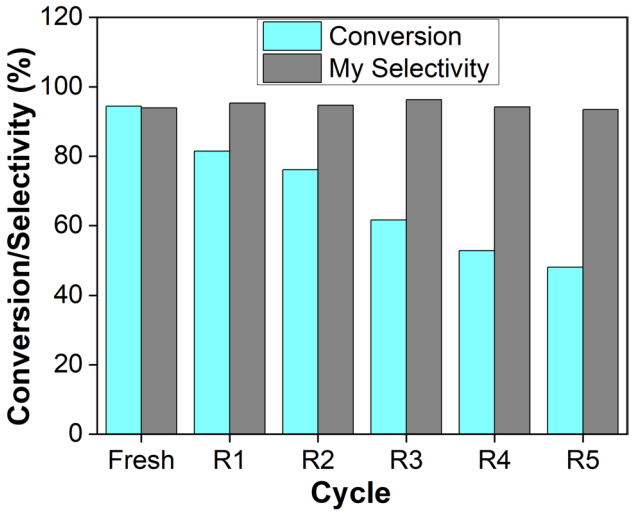


Figure 15 Reuse of CAT_400 catalyst in the isomerization of β-pinene epoxide. Reaction conditions: 75 mg catalyst, 90 °C, 0.25 mmol β -pinene epoxide, 750 rpm. The catalyst before reuses (Rx, with x the number of reuses) was washed with acetone and calcined at 400 °C (5 °C/min) for 2 h.

Characterization of reused catalyst

The acid strength of CAT_400 before and after five reuses was evaluated by TPD-NH_3. Figure S11 shows the experimental signal and the deconvolution of the respective peaks for each material; Table 9 shows the amount and type of acidity according to its strength. A decrease of acid sites of 51% and 47% of the CAT_400 catalyst was determined after five reuses in the isomerization of α- and β-pinene epoxide, respectively. The reduction of strong acid sites affects the conversion of α- and β-pinene epoxides.

Figure S12 shows that CAT_400 before and after five reuses presents the same mineralogical phases. However, the semi-quantitation of the phases obtained by Rietveld refinement of the diffractograms (Table 10) indicates that after reuse, hematite and rutile phases are transformed back into ilmenite; it has been reported that this is a reversible reaction.

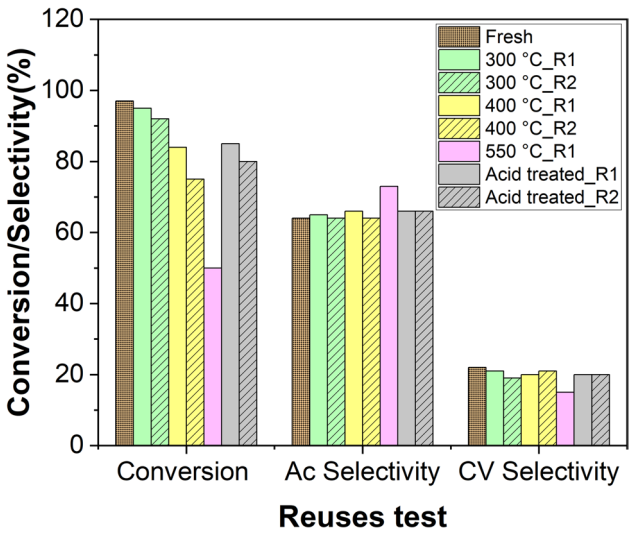


Figure 16 Reuse of CAT_400 catalyst in the isomerization of α-pinene epoxide. Reaction conditions: 100 mg catalyst, 90 °C, 0.25 mmol α-pinene epoxide, 750 rpm. The catalyst before reuse (Rx, with x the number of reuses) was washed with acetone and calcined (5 °C/min) at 300 (**a**) or 550 (**b**) °C for 2 h.

Table 9 Quantification of acid sites by NH_3-TPD ($\mu mol_{NH3}/g$)* of fresh and reused CAT_400 catalyst

Sample	Acidity		
	Low (100–220 °C)	Strong (400–600 °C)	Total
CAT_400	171	193	364
CAT_400a	141	38	179
CAT_400b	147	48	195

*The type of acidity was classified according to reference [53]. CAT_400a and CAT_400b are the catalysts after the fifth reuse in α-pinene epoxide and β-pinene isomerization

Table 10 Phase composition (%) of fresh and reused CAT_400 catalyst

Sample	Ilmenite	Hematite	Rutile
CAT_400	29.9	52.7	17.4
CAT_400a	56.1	29.0	14.9
CAT_400b	51.4	31.0	17.6

CAT_400a and CAT_400b are the catalysts after the fifth reuse in α-pinene epoxide and β-pinene isomerization

Furthermore, from these results it can be inferred that the active phases in the isomerization of α- and β-pinene epoxides are hematite (Fe_2O_3) and rutile (TiO_2) because the conversion of α- and β-pinene epoxides decreased when the amount of hematite and/or rutile diminished in the catalyst.

Conclusions

The isomerization of α- and β-pinene epoxides was carried out over heterogeneous catalysts synthesized from mining waste (black sands) by thermal treatments and hydrothermal reaction with H_2SO_4. The effect of solvent, temperature, amount of catalyst and time were analyzed. The characterization of the catalysts showed the presence of hematite (F_2O_3), ilmenite ($FeTiO_3$) and rutile (TiO_2) by XRD and Raman analysis. Both CAT_400 and CTT_800 catalysts showed only the presence of Lewis sites; however, CAT_400 showed the highest total and strong acidity. Although the two tested materials contained Fe and Ti, the iron concentration was higher in CAT_400, the material that showed the highest surface area, mesoporosity, and pore diameter. The best material for monoterpene epoxide isomerization was CAT_400, giving α-pinene epoxide conversion of 96% with campholenic aldehyde selectivity of 64% with cyclohexane as solvent; β-pinene epoxide conversion was 98% with myrtanal selectivity of 92% with dioxane as solvent. After five reuses of CAT_400 for α- and β-pinene epoxide isomerization, there were no changes neither for campholenic aldehyde nor myrtanal selectivity; the diminishing in hematite and strong acid sites concentration could be the cause of conversion decrease; a good procedure for catalyst activation is the treatment at 300 °C. Finally, mining waste as black sand is an alternative for the synthesis of active catalysts for the isomerization of monoterpene epoxides because it contains Fe and Ti.

Acknowledgements

The authors acknowledge to the Comité para el Desarrollo de la Investigación -CODI- of the Universidad de Antioquia (project 2022-50092); to the Universidad Nacional campus Medellín and to the Instituto Tecnológico Metropolitano ITM for the financial support to the project "Geocatalysis: valorization of ilmenite from mine wastes." Also, the authors acknowledge to Mineros Aluvial S.A.S. for the black sand samples.

Author contributions

Luis Fernando Valencia: Methodology. Investigation. Formal analysis. Data curation. Visualization. Writing—original draft. Aída Luz Villa: Resources. Funding acquisition. Supervision. Visualization. Writing—review & editing.

Funding

Open Access funding provided by Colombia Consortium. CODI-Universidad de Antioquia, Project 2022-50092, Geocatalysis: valorization of ilmenite from mine wastes, Universidad Nacional campus Medellín, the Instituto Tecnológico Metropolitano ITM, Mineros Aluvial S.A.S.

Data availability

The data that support this paper are available from the corresponding author upon request from readers.

Declarations

Conflict of interest The authors declare that they have no known competing financial interests or personal relationships that could have appeared to influence the work reported in this paper.

Supplementary Information The online version contains supplementary material available at https://doi.org/10.1007/s10853-025-11056-5.

Open Access This article is licensed under a Creative Commons Attribution 4.0 International License, which permits use, sharing, adaptation, distribution and reproduction in any medium or format, as long as you give appropriate credit to the original author(s) and the source, provide a link to the Creative Commons licence, and indicate if changes were made. The images or other third party material in this article are included in the article's Creative Commons licence, unless indicated otherwise in a credit line to the material. If material is not included in the article's Creative Commons licence and your intended use is not permitted by statutory regulation or exceeds the permitted use, you will need to obtain permission directly from the copyright holder. To view a copy of this licence, visit http://creativecommons.org/licenses/by/4.0/.

References

[1] Luo L, Wu H, Xu L, Meng J, Lu J, Zhou H, Huo X, Huang L (2021) An in situ ATR-FTIR study of mixed collectors BHA/DDA adsorption in ilmenite-titanaugite flotation system. Int J Min Sci Technol 31(4):689–697. https://doi.org/10.1016/J.IJMST.2021.05.001

[2] Cheng G, Gao Z, Yang S, Yang H, Xue X (2021) Microstructure and chemical transformation of natural ilmenite during isothermal roasting process in air atmosphere. Minerals 11(2):137. https://doi.org/10.3390/min11020137

[3] Joy M, Bhat H (2025) An overview of phase analysis and strategies on the development of acid soluble titania for sulphate process. Discov Chem 2:31. https://doi.org/10.1007/s44371-025-00110-5

[4] Zhou Z, Hua Y, Xu C, Li J, Li Y, Xiong L, Zhang Z (2017) Electrolytic synthesis of ferrotitanium powders from ilmenite in CaCl2-NaCl melts at a lower temperature of 700 °C. J Alloys Compd 726:1124–1131. https://doi.org/10.1016/j.jallcom.2017.08.102

[5] Teyssié G, Leion H, Schwebel GL, Lyngfelt A, Mattisson T (2011) Influence of lime addition to ilmenite in chemical-looping combustion (CLC) with solid fuels. Energy Fuels 25(8):3843–3853. https://doi.org/10.1021/ef200623h

[6] García-Muñoz P, Pliego G, Zazo JA, Bahamonde A, Casas JA (2015) Ilmenite ($FeTiO_3$) as low cost catalyst for advanced oxidation processes. J Environ Chem Eng 4(1):542–548. https://doi.org/10.1016/j.jece.2015.11.037

[7] Sánchez-Velandia JE, Pájaro E, Villa AL, Martínez-O F (2021) Selective synthesis of camphene from isomerization of α-and β-pinene over heterogeneous catalysts. Microporous Mesoporous Mater 324:111273. https://doi.org/10.1016/j.micromeso.2021.111273

[8] Sánchez-Velandia JE, Valdivieso LM, Martínez-O F, Mejía SM, Villa AL, Wärnå J, Murzin DY (2023) Synthesis of trans-pinocarveol from oxidation of β-pinene using multifunctional heterogeneous catalysts. Mol Catal 541:113104. https://doi.org/10.1016/j.mcat.2023.113104

[9] Sánchez-Velandia JE, Villa AL (2019) Isomerization of α-and β-pinene epoxides over Fe or Cu supported MCM-41 and SBA-15 materials. Appl Catal A: Gen 580:17–27. https://doi.org/10.1016/j.apcata.2019.04.029

[10] Gusevskaya EV (2014) Reactions of terpenes catalyzed by heteropoly compounds: valorization of biorenewables. ChemCatChem 6:1506–1515. https://doi.org/10.1002/cctc.201400052

[11] Sánchez-Velandia JE, Becerra JA, Mejía SM, Villa AL, Martínez-O F (2021) Thermodynamics of the isomerization of monoterpene epoxides. ACS Omega 6(50):34206–34218. https://doi.org/10.1021/acsomega.1c03049

[12] Chaves-Restrepo M, Viloria A, Sánchez-Velandia JE, Villa AL (2022) Effect of reaction conditions and kinetics of the isomerization of β-pinene epoxide to myrtanal in the presence of Fe/MCM-41 and Fe/SBA-15. React Kinet Mech Catal 135:2013–2029. https://doi.org/10.1007/s11144-022-02220-y

[13] Stekrova M, Kumar N, Díaz SF, Mäki-Arvela P, Murzin DY (2015) H-and Fe-modified zeolite beta catalysts for preparation of trans-carveol from-pinene oxide. Catal Today 241:237–245. https://doi.org/10.1016/j.cattod.2013.12.004

[14] Salminen E, Mäki-Arvela P, Vitanen P, Salmi T, Wärnå J, Mikkola JP (2014) Kinetics upon isomerisation of αβ-pinene oxides over supported ionic liquid catalysts (silcas) containing lewis acids kinetics upon isomerisation of αβ-pinene oxides over supported ionic liquid catalysts (SILCAs) containing lewis acids. Ind Eng Chem Res 53(52):20107–20115

[15] Sánchez JE, Villa AL (2022) Selective synthesis of high-added value chemicals from α-pinene epoxide and limonene epoxide isomerization over mesostructured catalysts: effect of the metal loading and solvent. Catal Today 394–396:208–218. https://doi.org/10.1016/j.cattod.2021.09.011

[16] Stekrova M, Kumar N, Aho A, Sinev I, Grünert W, Dahl J, Roine J, Arzumanov SS, Mäki-Arvela P, Murzin DY (2014) Isomerization of-pinene oxide using Fe-supported catalysts: selective synthesis of campholenic aldehyde. Appl Catal A: Gen 470:162–176. https://doi.org/10.1016/j.apcata.2013.10.044

[17] Pitínová M, Eliášová P, Weissenberger T, Shamzhy M, Musilová Z, Čejka J (2018) Highly selective synthesis of campholenic aldehyde over Ti-MWW catalysts by α-pinene oxide isomerization. Catal Sci Technol 8(18):4690–4701. https://doi.org/10.1039/C8CY01231H

[18] Demidova YS, Ardashov OV, Simakova OA, Simakova IL, Volcho KP, Salakhutdinov NF, Murzin DY (2014) Isomerization of bicyclic terpene epoxides into allylic alcohols without changing of the initial structure. J Mol Catal A Chem 388–389:162–166. https://doi.org/10.1016/J.MOLCATA.2013.09.016

[19] Coelho JV, de Meireles AL, da Silva Rocha KA, Pereira MC, Oliveira LC, Gusevskaya EV (2012) Isomerization of-pinene oxide catalyzed by iron-modified mesoporous silicate. Appl Catal A: Gen 443:125–132. https://doi.org/10.1016/j.apcata.2012.07.030

[20] Bruno SM, Gomes AC, Gamelas CA, Abrantes M, Olivera MC, Valente AA, Almeida FA, Pillinger M, Romao CC, Gonçalves IS (2014) Application of an indenyl molybdenum dicarbonyl complex in the isomerisation of a-pinene oxide to campholenic aldehyde. New J Chem 38:3172–3180. https://doi.org/10.1039/C4NJ00371C

[21] Vyskočilová E, Lhotka M, Červený L (2020) Solvent influence on selectivity in α-pinene oxide isomerization using MoO3-modified zeolite BETA. Catal 10(11):1–17. https://doi.org/10.3390/catal10111244

[22] Sidorenko AY, Kravtsova AV, Aho A, Heinmaa I, Kuznetsova TF, Murzin DY, Agabekov VE (2018) Catalytic isomerization of A-pinene oxide in the presence of acid-modified clays. Mol Catal 448:18–29. https://doi.org/10.1016/j.mcat.2018.01.021

[23] Costa V, da Silva RK, de Sousa LF, Robles PA, Gusevskaya EV (2011) Isomerization of α-pinene oxide over cerium and tin catalysts: Selective synthesis of trans-carveol and trans-sobrerol. J Mol Catal A Chem 345:69–74. https://doi.org/10.1016/j.molcata.2011.05.020

[24] Advani JH, Singh AM, Khan NH, Bajaj HC, Biradar AV (2020) Black yet green: Sulfonic acid functionalized carbon as an efficent catalyst for highly selective isomerization of α-pinene oxide to trans-carveol. Appl Catal B: Environ 268:118456. https://doi.org/10.1016/j.apcatb.2019.118456

[25] da Silva Rocha KA, Hoehne JL, Gusevskaya EV (2008) Phosphotungstic acid as a versatile catalyst for the synthesis of fragrance compounds by a-pinene oxide isomerization: solvent-induced chemoselectivity. Chem Eur J 14(20):6166–6172. https://doi.org/10.1002/chem.200800184

[26] Costa VV, da Silva Rocha KA, de Sousa LF, Robles PA, Gusevskaya EV (2011) Isomerization of -pinene oxide over cerium and tin catalysts: selective synthesis of trans-carveol and trans-sobrerol. J Mol Catal A Chem 345:69–74. https://doi.org/10.1016/j.molcata.2011.05.020

[27] Barakov R, Shcherban N, Maki-Arvela P, Yaremov P, Bezverkhyy I, Wärnå J, Murzin DY (2022) Hierarchical beta zeolites as catalysts in α-pinene oxide isomerization. ACS Sustain Chem Eng 10(20):6642–6656. https://doi.org/10.1021/acssuschemeng.2c00441

[28] Stekrova M, Kumar N, Díaz SF, Mäki-Arvela P, Murzin DY (2015) H-and Fe-modified zeolite beta catalysts for preparation of trans-carveol from α-pinene oxide. Catal Today 241:237–245. https://doi.org/10.1016/j.cattod.2013.12.004

[29] Cruz MC, Sánchez-Velandia JE, Causíl S, Villa AL (2021) Selective synthesis of perillyl alcohol from β-pinene epoxide over Ti and Mo supported catalysts. Catal Letters 151:2279–2290. https://doi.org/10.1007/s10562-020-03489-1

[30] De La Torre O, Renz M, Corma A (2010) Biomass to chemicals: rearrangement of β-pinene epoxide into myrtanal with well-defined single-site substituted molecular sieves as reusable solid Lewis-acid catalyst. Appl Catal A: Gen 380:165–171. https://doi.org/10.1016/j.apcata.2010.03.056

[31] Vyskočilová E, Maly M, Aho A, Krupka J, Červený L (2016) The solvent effect in b-pinene oxide rearrangement.

React Kinet Mech Catal 118:235–246. https://doi.org/10.1007/s11144-016-0994-9

[32] Vyskočilová E, Dušek J, Babirádová M, Krupka J, Paterová I, Červený L (2018) Perillyl alcohol preparation from β-pinene oxide using Fe-modified zeolite beta. Res Chem Intermed 44(7):3971–3984. https://doi.org/10.1007/s11164-018-3335-y

[33] Valencia LF, Agudelo I, Badano J, Quiroga M, Betti C, Lederho C, Villa AL (2025) Zn supported on composite materials as catalysts for fine chemical applications. Mol Catal 578:115012. https://doi.org/10.1016/j.mcat.2025.115012

[34] Pratika RA, Wijaya K, Trisunaryanti W (2021) Hydrothermal treatment of SO_4/TiO_2 and TiO_2/CaO as heterogeneous catalysts for the conversion of Jatropha oil into biodiesel. J Environ Chem Eng 9(6):106547. https://doi.org/10.1016/j.jece.2021.106547

[35] Thommes M, Kaneko K, Neimark A, Olivier J, Rodriguez F, Rouquerol J, Sing K (2015) Physisorption of gases with special reference to the evaluation of surface area and pore size distribution (IUPAC technical report). Pure Appl Chem 87(9–10):1051–1069. https://doi.org/10.1515/pac-2014-1117

[36] Sánchez-Velandia JE, Gelves JF, Dorkis L, Márquez MA, Villa AL (2019) Ring-opening of β-pinene epoxide into high-added value products over Colombian natural zeolite. Microporous Mesoporous Mater 287:114–123. https://doi.org/10.1016/j.micromeso.2019.05.053

[37] Sánchez-Velandia JE, Gelves JF, Márquez MA, Dorkis L, Villa AL (2020) Catalytic isomerization of α-pinene epoxide over a natural zeolite. Catal Letters 150:3132–3148. https://doi.org/10.1007/s10562-020-03225-9[

[38] Fu X, Wang Y, Wei F (2010) Twin nucleation by slip transfer across grain boundaries in commercial purity titanium. Metall Mater Trans A 44:1338–1348. https://doi.org/10.1007/s11661-009-0097-6

[39] Zhang X, Du Z, Zhu Q, Li J, Xie Z (2022) Enhanced reduction of ilmenite ore by pre-oxidation in the view of pore formation. Powder Technol 405:11753. https://doi.org/10.1016/j.powtec.2022.117539

[40] Mohamad NA, Hamzah S, Che-Harun MH, Ali A, Rasit N, Awang M, Abdul-Raham WR, Rahman-Azmi AA, Amri-Zahid MS, Fahmi-Mustofa AA, Ahmed-Latfi S, Aripin SM, Saad R (2022) Copperas as iron-based coagulant for water and wastewater treatment: a review. Biointerface Res Appl Chem 12(3):4155–4176. https://doi.org/10.33263/BRIAC123.41554176

[41] Reshetenko TV, Avdeeva LB, Khassin AA, Kustova GN, Ushakov VA, Moroz EM, Shmakov AN, Kriventsov VV, Kochubey DI, Pavlyukhin YT, Chuvilin AL, Ismagilov ZR (2004) Coprecipitated iron-containing catalysts (Fe-Al_2O_3, Fe-Co- Al_2O_3, Fe-Ni- Al_2O_3) for methane decomposition at moderate temperatures I. genesis of calcined and reduced catalysts. Appl Catal A: Gen 268:127–138. https://doi.org/10.1016/j.apcata.2004.03.045

[42] Kaleeswarran P, Kumar MP, Mangalaraja RV, Hartley UW, Sasikumar M, Venugopalan R, Kumar MR, Rajabathar JR, Peera SG, Murugadoss G (2021) $FeTiO_3$ perovskite nanoparticles for efficient electrochemical water splitting. Catal 11(9):1028. https://doi.org/10.3390/catal11091028

[43] Nair VS, Kokulnathan T, Wang TJ, Vishnuraj R, Dinesh H, Rangarajan M (2024) Hydrothermal synthesis of iron titanate hexagonal nanoplates for electrochemical detection of nitrofurazone. Mikrochim Act 191(5):245. https://doi.org/10.1007/s00604-024-06300-9

[44] Humayun A, Manivelan N, Prabakar K (2024) Charge transfer in n-FeO and p-α-Fe_2O_3 nanoparticles for efficient hydrogen and oxygen evolution reaction. Nanomater 14(18):1515. https://doi.org/10.3390/nano14181515

[45] Zhang ST, Ruan YR, Liu C, Wang P, Ma YQ (2017) The evolution of structure, chemical state and photocatalytic performance of α-Fe/$FeTiO_3/TiO_2$ with the nitridation at different temperatures. Mater Res Bull 95:503–508. https://doi.org/10.1016/j.materresbull.2017.08.042

[46] Escobar L, Solis DA, Romero S, Haro E (2024) TiO_2-Fe_2O_3 nanocomposite thin films prepared by magnetron sputtering for photocatalytic applications. Mater Sci Eng: B 302:117261. https://doi.org/10.1016/j.mseb.2024.117261

[47] Rani C, Pathak DK, Tanwar M, Kandpal S, Chosh T, Maximov MY, Kumar R (2022) Anharmonicity induced faster decay of hot phonons in rutile TiO_2 nanorods: a Raman spectromicroscopy study. Mater Adv 3:1602–1608. https://doi.org/10.1039/D1MA00940K

[48] Imperial A, Pe-Piper G, Piper D, Grey L (2022) Identifying pseudorutile and kleberite using Raman spectroscopy. Minerals 12(10):1210. https://doi.org/10.3390/min12101210

[49] Reyes V, León JI, Hernandez E, Perez S, Hurtado LA, Landeros B (2020) Synthesis and characterization of magnetite nanoparticles for photocatalysis of nitrobenzene. J Saudi Chem Soc 24(2):223–235. https://doi.org/10.1016/j.jscs.2019.12.004

[50] Jayalath G, Nishadini UGT, Wickramasooriya HMBN, Subasinghe HCS, Sandaruwan A (2024) Effect of mechanical activation and HNO_3 pre-treatment of Pulmoddai ilmenite for the extraction of Ti and TiO_2 using H_2SO_4, HCl, and KOH-assisted leaching. Hydrometallurgy 226:106314. https://doi.org/10.1016/j.hydromet.2024.106314

[51] Adzahar NA, Asikin N, Izham M, Abdulkareem G, Mastuli MS, Razali M, Taufiq-Yap YH (2022) Chemoselective decarboxylation of ceiba oil to diesel-range alkanes over a

red mud based catalyst under H_2-free conditions. RSC Adv 12:16903–16917. https://doi.org/10.1039/D2RA00853J

[52] Boz I, Boroglu MS, Zengin Y, Kaya B (2023) Sustainable production of acrolein over highly stable and selective WO_3 over SiO_2-TiO_2 catalysts. Korean J Chem Eng 40(8):1882–1891. https://doi.org/10.1007/s11814-023-1406-2

[53] Kaya B, Zengin Y, Safak M, Boz I (2023) Selective dehydration of glycerol to acrolein over mesoporous WO_3-KIT-6: effects of mesoporosity and acidity. J Porous Mater 30:835–845. https://doi.org/10.1007/s10934-022-01384-1

[54] Pitínová M, Eliášová P, Weissenberger T, Shamzhy M, Musilová Z, Čejka J (2018) Highly selective synthesis of campholenic aldehyde over Ti-MWW catalysts by α-pinene oxide isomerization. Catal Sci Technol 8(18):46904701. https://doi.org/10.1039/C8CY01231H

[55] Busch OM, Brijoux W, Thomson S, Schüth F (2004) Spatially resolving infrared spectroscopy for parallelized characterization of acid sites of catalysts via pyridine sorption: possibilities and limitations. J Catal 222(1):174–179. https://doi.org/10.1016/j.jcat.2003.11.002

[56] Li X, Zhang J, Liu B, Liu J, Wang C, Chen G (2019) Hydrodeoxygenation of lignin-derived phenols to produce hydrocarbons over Ni/Al-SBA-15 prepared with different impregnants. Fuel 243:314–321. https://doi.org/10.1016/j.fuel.2019.01.126

[57] Gil A (2023) Classical and new insights into the methodology for characterizing adsorbents and metal catalysts by chemical adsorption. Catal Today 423:114016. https://doi.org/10.1016/j.cattod.2023.01.023

[58] Penkova A, Bobadilla LF, Romero-Sarria F, Centeno MA, Odriozola JA (2014) Pyridine adsorption on NiSn/MgO–$Al2O_3$: An FTIR spectroscopic studyof surface acidity. Appl Surf Sci 317:241–251. https://doi.org/10.1016/j.apsusc.2014.08.093

[59] Maronna MM, Kruissink EC, Parton RF, Soulimani F, Weckhuysen BM, Hoelderich WF (2016) Spectroscopic study on the active site of a SiO2 supported niobia catalyst used for the gas-phase Beckmann rearrangement of cyclohexanone oxime to e-caprolactam. Phys Chem Chem Phys 18:22636–22646. https://doi.org/10.1039/c6cp03014a

[60] Boekaerts B, Lorenz W, Aelst V, Sels BF (2022) Kinetics of fatty acid ketonization in liquid phase with anatase and rutile TiO2 catalysts. Appl Catal B: Environ 305:121052. https://doi.org/10.1016/j.apcatb.2021.121052

[61] Miller SJ, Lacheen HJ, Chen CY (2016) Determining the strength of brønsted acid sites for hydrodewaxing over shape selective catalysts. Ind Eng Chem Res 55:1–27. https://doi.org/10.1021/acs.iecr.6b01081

[62] Mäki-Arvela P, Shcherban N, Lozachmeur C, Russo V, Wärnå J, Murzin DY (2019) Isomerization of α-pinene oxide: solvent effects. Kinet Thermodyn Catal Lett 149:203–214. https://doi.org/10.1007/s10562-018-2617-8

[63] Vyskočilová E, Hašková L, Červený L (2019) Solvent-induced selectivity in α-pinene oxide isomerization catalyzed by Fe-modified zeolite beta. Chem Pap 73:1621–1627. https://doi.org/10.1007/s11696-019-00713-0

[64] Singh A, Naikwadi D, Ravi K, Biradar A (2022) Chemoselective isomerization of α-Pinene oxide to *trans*-Carveol by robust and mild Brønsted acidic zirconium phosphate catalyst. Mol Catal 521:112189. https://doi.org/10.1016/j.mcat.2022.112189

[65] Mäki-Arvela P, Kumar N, Díaz SF, Aho A, Tenho M, Salonen J, Leino AR, Kordás K, Laukkanen P, Dahl J, Sinev I, Salmin T, Murzin DY (2013) Isomerization of β-pinene oxide over Sn-modified zeolites. J Mol Catal A Chem 366:228–237. https://doi.org/10.1016/j.molcata.2012.09.028

[66] Sánchez-Velandia JE, Agudelo-Cifuentes A, Villa AL (2019) Kinetics of the isomerization of α-pinene epoxide over Fe supported MCM-41 and SBA-15 materials. React Kinet Mech Catal 128(2):1005–1028. https://doi.org/10.1007/s11144-019-01656-z

Publisher's Note Springer Nature remains neutral with regard to jurisdictional claims in published maps and institutional affiliations.